

Multi-level hermite variational interpolation and quasi-interpolation

Shengjun Liu · Guido Brunnett · Jun Wang

Published online: 20 April 2013
© Springer-Verlag Berlin Heidelberg 2013

Abstract Based on the Hermite variational implicit surface reconstruction presented in Pan et al. (Science in China Series F: Information Sciences 52(2):308–315, 2009), we propose a multi-level interpolation method to overcome the problems resulted from using compactly supported radial basis functions (CSRBFs). In addition, we present a multi-level quasi-interpolation method which directly uses normal vectors to construct non-zero constraints and avoids solving any linear system, a common step of variational surface reconstruction, and leads to a fast and stable surface reconstruction from scattered points. With adaptive support size, our approach is robust and can successfully reconstruct surfaces on non-uniform and noisy point sets. Moreover, as the computation of quasi-interpolation is independent for each point, it can be easily parallelized on multi-core CPUs.

Keywords Interpolation · Quasi-interpolation · Hermite · Multi-level

1 Introduction

As the three-dimensional scanning devices are commonplace, there are more and more point data available from scanning the real world object by acquisition devices. In order to do further processing on the scattered points, surfaces are usually reconstructed from the points. A lot of research works have been devoted to develop reconstruction methods for applications in computer graphics, robotics, and computer-aided design and manufacturing (CAD/CAM) [1, 31].

Due to implicit surface modeling being good at dealing with noisy and/or incomplete data, there are many developments in this field. In those works, there are several surface reconstruction methods based on Radial Basis Functions (RBFs) [2–6]. Global RBFs [2, 3] are useful in repairing incomplete data, while a dense linear system needs to be solved. It is impractical for large point data although sophisticated mathematical techniques such as the fast multipole method [2] are used. Fitting scattered data with compactly supported radial basis functions (CSRBFs) [7] leads to a simpler and faster computation procedure [4–6]. The approaches based on CSRBFs are sensitive to the density of scattered data, therefore, a careful selection of the support size for CSRBFs is required to balance the reconstructed surface quality and reconstructing performance. A multi-level fitting technique presented in [5] provides a global property for the CSRBFs, while an extra local quadratic fitting is required at each level. Recently, Pan et al. proposed a Hermite variational implicit surface (HVIS) reconstruction method which uses the normal information of points directly instead of local quadratic approximations [6]. But when using CSRBF as the kernel function, it yields unwanted artifacts in addition to the lack of extrapolation across holes. In this paper, we presented a hierarchical HVIS reconstruc-

S. Liu (✉)
School of Mathematics and Statistics, Central South University,
Changsha 410083, China
e-mail: shjliu.cg@csu.edu.cn

G. Brunnett
Department of Computer Science, Chemnitz University
of Technology, Chemnitz 09107, Germany
e-mail: Guido.Brunnett@informatik.tu-chemnitz.de

J. Wang
College of Mechanical and Electrical Engineering, Nanjing
University of Aeronautics and Astronautics, Nanjing 210016,
China
e-mail: davis.wjun@gmail.com

tion method which has the advantage of globally supported RBFs and is robust on incomplete or non-uniform points.

For all reconstruction methods based on RBFs mentioned above, solving a linear system is required. When there are a large number of points, the interpolation matrix may become ill-conditioned. This leads to unstable numerical computation and a high computational cost. Comparing with an exact interpolation approach, the quasi-interpolation method presented in this paper does not solve any linear systems, and can reconstruct satisfactory surfaces with small shape approximation errors.

The main contributions of this work include three aspects. Firstly, we present a multi-level HVIS reconstruction method which provides advantages of locally and globally supported RBFs by using CSRBFs in a hierarchical way. Secondly, a quasi-interpolation scheme is introduced for fitting scattered points. It does not solving linear systems. The reconstruction in that the RBF on each point is computed locally and independently can be easily parallelized. Lastly, an adaptive strategy for choosing local supports in CSRBFs-based fitting is used for reconstructing surfaces from highly non-uniform points. A threshold of nearest neighbor number needs to be set by users for determining adaptive support radius.

The rest of this paper is organized as follows. After reviewing some related works in Sect. 2, we describe the HVIS reconstruction method in brief in Sect. 3. Then, a multi-level HVIS reconstruction method is presented in Sect. 4. Section 5 presents the details about quasi-interpolation and adaptive support size choosing. The conclusion section follows the experimental results given in Sect. 6.

2 Related works

Surface reconstruction from points has been an important procedure in geometric modeling for a few decades. A number of reconstruction algorithms proposed can be roughly classified into two major groups as follows.

Explicit methods Many algorithms usually involve Voronoi diagram construction and reconstruct a mesh surface by linking the points directly [8–11]. This type of methods are more sensitive to the point set quality, such as distribution, noise etc. than implicit methods. Moreover, the cost to compute Voronoi diagram is expensive in both memory and time.

Implicit methods The algorithms in this group attempt to create a signed implicit function, which divides the space into inside and outside of an object, from a set of oriented points, such as RBF-based approaches [2–6, 12–14], integration of Voronoi diagrams and variational method [15],

Poisson surface reconstruction technique [16], smooth signed distance method [17], piecewise linear surfaces [18], moving least squares-based [19–21], and partition of unity-based method [22].

Our work is based on the HVIS reconstruction [6], in which CSRBFs used form a sparse linear system, and a hierarchy of using CSRBFs is created to achieve a global function. In [6], directly using normal vectors in the implicit function leads to a much less $n \times n$ positive definite linear system for given points with normals, while the variational implicit surface [2, 12] results in a $2n \times 2n$ system by inserting off-surface points and the interpolating normal vectors method [13, 14] gives a $4n \times 4n$ system. Our multi-level HVIS is similar to the work in [5], but the latter combines the partition of unity (PU) and RBFs, and local quadratic approximations are used for non-zero valued constraints instead of using normal vectors directly.

In addition, our surface reconstruction method presented in this paper applies a quasi-interpolation scheme to speed up the reconstruction of surfaces from scattered points. It does not solve linear systems so that it is stable and efficient. The adaptive multi-level quasi-interpolation framework is robust to points with non-uniformities, and can successfully reconstruct surfaces in high quality.

Quasi-interpolation Quasi-interpolation methods have been discussed for a long time in the field of function approximation of a function [23–25]. It possesses some advantages, such as less computation time and stable computation. In [26], Zhang and Wu discussed the univariate quasi-interpolants. A quasi-interpolation method based on radial basis functions is discussed, and a suitable value of the shape parameter is provided in [27]. The data the former methods processed are a kind of regularly sampled grid points. In [28], Liu et al. generalize the data to 3D scattered points, and get good reconstruction results. However, their method is based on the PU and RBF interpolation method [5], in which solving small linear systems is necessary for local quadratic fitting. The surface reconstruction method in this paper is faster than the one in [28] because it uses normal vectors directly without solving any linear system.

3 Review of HVIS reconstruction

Given a set V of n data triplets $(\mathbf{v}_i, \mathbf{n}_i, f_i)$, $i = 1, \dots, n$, where $\mathbf{v}_i \in \mathbb{R}^3$ are 3D points, $\mathbf{n}_i \in \mathbb{R}^3$ are the corresponding normal vectors, and $f_i \in \mathbb{R}$ are their associated signed distances, we want to fit a function $f(\mathbf{x})$ to them. Since the normal direction of the implicit surface is given by the gradient $\nabla f(\mathbf{x})$ of the embedding function $f(\mathbf{x})$, the normal vectors, \mathbf{n}_i at the given points can be directly incorporated

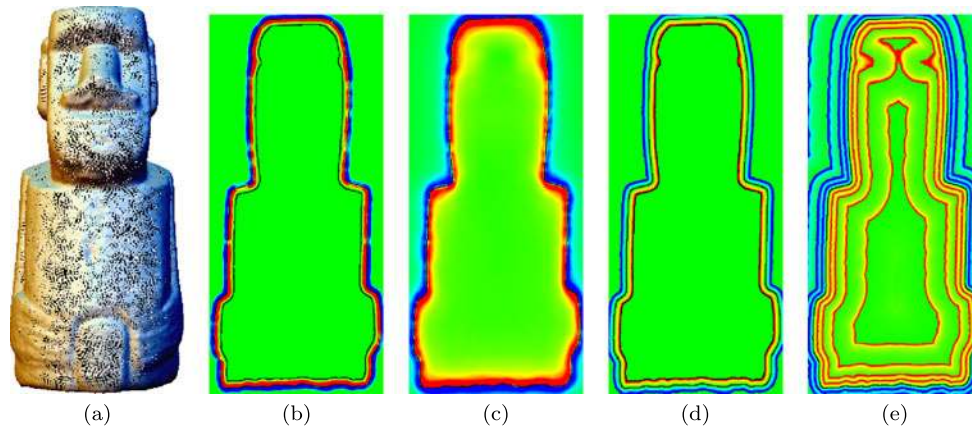


Fig. 1 Comparisons of the cross sections of signed distance fields generated by single-level and multi-level Hermite variational implicit surface interpolation and quasi-interpolation methods: (a) the given points, (b) single-level Hermite variational interpolation with CSRBFs [6], (c) multi-level Hermite variational interpolation,

(d) single-level Hermite variational quasi-interpolation, (e) multi-level Hermite variational quasi-interpolation. The colors show the function values (red for positive value, blue for negative value), the black curve highlights its zero iso-curve and the green color shows the undefined region

into an optimization problem [6] by

$$E(f) = \|f\|_H^2 + k_1 \sum_{j=1}^n (f(\mathbf{v}_j) - f_j)^2 - k_2 \sum_{j=1}^n \langle \mathbf{n}_j, \nabla f(\mathbf{v}_j) \rangle, \quad (1)$$

where k_1, k_2 are positive parameters to weigh between fitness to the data points/normals and smoothness of the surface, $\langle \cdot, \cdot \rangle$ denotes the dot-product of two vectors, the norm $\|f\|_H$ is a regularizer that takes on larger values for less smooth functions, and H is a reproducing kernel Hilbert space with kernel function $\phi(\cdot)$.

The final solution to the problem Eq. (1) is [6]

$$f(\mathbf{x}) = \sum_{j=1}^n c_j \phi(\|\mathbf{x} - \mathbf{v}_j\|) + \sum_{j=1}^n \langle \mathbf{n}_j, \nabla \phi(\|\mathbf{x} - \mathbf{v}_j\|) \rangle, \quad (2)$$

where the coefficients, c_i , are unknown scales to be determined by the interpolation constraints, $f(\mathbf{v}_i) = f_i, i = 1, \dots, n$. Because the surface defined by points with normals, $(\mathbf{v}_i, \mathbf{n}_i)$, is always expected to be a zero level set in a distance field of a signed function, the constraints become $f(\mathbf{v}_i) = 0, i = 1, \dots, n$, as is

$$\sum_{j=1}^n c_j \phi(\|\mathbf{v}_i - \mathbf{v}_j\|) + \sum_{j=1}^n \langle \mathbf{n}_j, \nabla \phi(\|\mathbf{v}_i - \mathbf{v}_j\|) \rangle = 0.$$

The above equation can be rewritten as

$$\sum_{j=1}^n c_j \phi(\|\mathbf{v}_i - \mathbf{v}_j\|) = - \sum_{j=1}^n \langle \mathbf{n}_j, \nabla \phi(\|\mathbf{v}_i - \mathbf{v}_j\|) \rangle. \quad (3)$$

The right side of Eq. (3) is non-zero. So, when we use a positive definite CSRBF as the kernel function ϕ , the coefficients c_i can be determined uniquely by solving the sparse linear system Eq. (3).

4 Multi-level HVIS interpolation

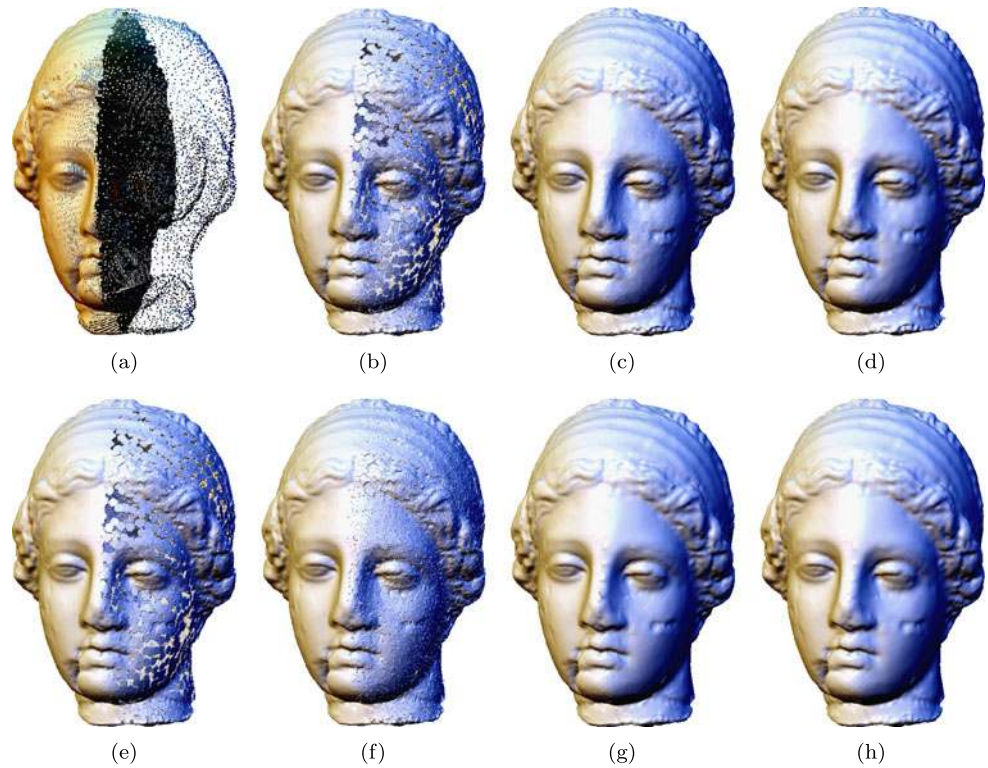
In this paper, we use Wendland's CSRBF [7] as the kernel function

$$\phi_\rho = \phi(r/\rho), \quad \phi(r) = \begin{cases} (1-r)^4(4r+1), & r \in [0, 1], \\ 0, & \text{otherwise,} \end{cases}$$

where ρ is the support size, and $r = \|\mathbf{p} - \mathbf{q}\|$ is the Euclidean distance between a point \mathbf{p} and a RBF center \mathbf{q} . As stated in [6], using CSRBFs in HVIS reconstruction cannot repair incomplete data in addition to generate extra unwanted zero level-set surface at the boundary of the supporting field, as shown in Figs. 1(b) and 2(b). Moreover, an implicit surface reconstructed by single-level CSRBFs only has valid function values defined in a narrow band around the surface. Therefore, the grids used for polygonization need to be smaller than the support size. This further slows the procedure of mesh surface generation.

In order to overcome the problems, we borrow the idea of constructing multi-level interpolation in [5]. We build a multi-scale hierarchy $\{V^1, V^2, \dots, V^M = V\}$ of point sets by subdividing the points of V into eight equal octants recursively. For each cell, the centroid of all points located in this cell is computed and assigned with the unit average normal determined from these points. The centroids of cells in level k are considered as points in a set V^k . New RBFs at different levels are iteratively added to refine the fitting results.

Fig. 2 Reconstruction results with different methods: (a) given non-uniform points, (b) single-level Hermite variational interpolation, (c) multi-level Hermite variational interpolation, (d) multi-level Hermite variational interpolation with adaptive support size, $\sigma = 10$, (e) and (f) single-level and multi-level Hermite variational quasi-interpolation, (g) and (h) single-level and multi-level Hermite variational quasi-interpolation with adaptive support size, $\sigma = 10$



We define a series of functions according to the hierarchy of point sets

$$\begin{cases} f^0(\mathbf{x}) = 0, \\ f^k(\mathbf{x}) = f^{k-1}(\mathbf{x}) + \delta^k(\mathbf{x}), \quad k = 1, 2, \dots, M, \end{cases}$$

where $f^k(\mathbf{x}) = 0$ interpolates the point set V^k . The offsetting function between the functions of two adjacent levels is defined by a form presented in Sect. 3 for the single-level interpolation as

$$\delta^k(\mathbf{x}) = \sum_{j=1}^{n^k} c_j^k \phi_{\rho^k}(\|\mathbf{x} - \mathbf{v}_j^k\|) + \sum_{j=1}^{n^k} \langle \mathbf{n}_j^k, \nabla \phi(\|\mathbf{x} - \mathbf{v}_j^k\|) \rangle,$$

where n^k is the point number of V^k , \mathbf{n}_j^k is the normal vector of point \mathbf{v}_j^k , and ρ^k is the support radius at the level k . The coefficients, c_j^k , are determined by solving the following system of linear equations:

$$\begin{aligned} & \sum_{j=1}^{n^k} c_j^k \phi_{\rho^k}(\|\mathbf{v}_i^k - \mathbf{v}_j^k\|) \\ &= -f^{k-1}(\mathbf{v}_i^k) - \sum_{j=1}^{n^k} \langle \mathbf{n}_j^k, \nabla \phi_{\rho^k}(\|\mathbf{v}_i^k - \mathbf{v}_j^k\|) \rangle, \\ & i = 1, \dots, n^k. \end{aligned} \quad (4)$$

Here, we adopt the strategy in [5] to compute the support size ρ^k and the clustering levels M . The support size ρ^k at the level k is recursively defined by $\rho^{k+1} = \rho^k/2$ and $\rho^1 = \alpha L$, where L is the diagonal length of the bounding box of V , and the parameter $\alpha = 0.75$ is chosen such that an octant of the bounding box is always covered by a ball of radius ρ^1 centered somewhere in the octant. With the equation $M = \lceil -\log_2(\hat{\rho}/(2\rho^1)) \rceil$ provided in [5], the number of levels, M , can be determined by ρ^1 and $\hat{\rho}$, where $\hat{\rho}$ is equal to $3/4$ of the average diagonal length of the leaf cells, which contain not more than eight points of V . The multi-level HVIS makes that the final interpolation function defines a global distance field and fills the holes in the given points, as shown in Figs. 1(c) and 2(c).

5 Quasi-interpolation

The multi-level HVIS can reconstruct good quality surface from scattered points by solving a $n^k \times n^k$ sparse linear system at k level. However, solving a linear system still limits the number of points. The linear system may be ill-conditioned and its solving is computational costly as the points increase more and more. In this section, we introduce a quasi-interpolation scheme to fit the given points in a stable and efficient way.

The early quasi-interpolation traces back to [32] in which a surface interpolating a given data set can be represented by

a weighted average of the values at the data points. Shepard successfully constructed a group of weighting functions to approximate interpolate two-dimensional data. We can use the idea to fit 3D scattered points as follows:

$$\tilde{g}(\mathbf{x}) = \sum_{i=1}^n f_i \varphi_i(\mathbf{x}), \quad (5)$$

where $\varphi_i(\mathbf{x})$ s are the normalized radial basis functions $\varphi_i(\mathbf{x}) = \phi_\rho(\|\mathbf{x} - \mathbf{v}_i\|) / \sum_{j=1}^n \phi_\rho(\|\mathbf{x} - \mathbf{v}_j\|)$.

For given points, we consider an interpolant $g(\mathbf{x})$ as

$$g(\mathbf{x}) = \sum_{i=1}^n c_i \varphi_i(\mathbf{x}). \quad (6)$$

Comparing two equations Eq. (5) and Eq. (6), when the coefficients, c_i , are set as

$$c_i = f_i \quad (i = 1, \dots, n), \quad (7)$$

the interpolating function $g(\mathbf{x})$ is approximated by $\tilde{g}(\mathbf{x})$. However, unlike two-dimensional interpolation in [32], the values, f_i , at 3D data points are unknown for surface reconstruction. Generally, we assume the values, f_i , being zero in order to make all given 3D points locating on the zero level-set in a distance field defined by an implicit function. This leads to a trivial solution that the function is zero everywhere for either interpolation Eq. (6) or quasi-interpolation Eq. (5). The methods constructing non-zero valued constraints using the normal vectors directly are described in [6] and Sect. 4 for interpolation. In this section, we demonstrate how to construct non-zero valued constraints and use them to quasi-interpolation.

5.1 Single-level quasi-interpolation

For the interpolation problem, using a normalized or non-normalized basis does not affect the reconstruction results. So, Eq. (2) can be written with a normalized basis as

$$f(\mathbf{x}) = \sum_{j=1}^n c_j \varphi_j(\mathbf{x}) + \sum_{j=1}^n \langle \mathbf{n}_j, \nabla \varphi_j(\mathbf{x}) \rangle.$$

For exact interpolation, the coefficients, c_i , are determined by solving the system of linear equations

$$g(\mathbf{x}) = \sum_{j=1}^n c_j \varphi_j(\mathbf{x}) = - \sum_{j=1}^n \langle \mathbf{n}_j, \nabla \varphi_j(\mathbf{x}) \rangle.$$

Let $g_i = - \sum_{j=1}^n \langle \mathbf{n}_j, \nabla \varphi_j(\mathbf{v}_i) \rangle$ be the value of the function $g(\mathbf{x})$ at point \mathbf{v}_i , with the above analysis of quasi-interpolation, the values of the coefficients, c_i , can be found

by

$$c_i = - \sum_{j=1}^n \langle \mathbf{n}_j, \nabla \varphi_j(\mathbf{v}_i) \rangle, \quad i = 1, \dots, n, \quad (8)$$

then the quasi-solution $\tilde{f}(\mathbf{x})$ of the interpolation function $f(\mathbf{x})$ can be constructed as

$$\tilde{f}(\mathbf{x}) = \sum_{i=1}^n \left(- \sum_{j=1}^n \langle \mathbf{n}_j, \nabla \varphi_j(\mathbf{v}_i) \rangle \right) \varphi_i(\mathbf{x}) + \sum_{i=1}^n \langle \mathbf{n}_i, \nabla \varphi_i(\mathbf{x}) \rangle. \quad (9)$$

5.2 Multi-level quasi-interpolation

The computation of the above quasi-interpolation is very fast as the evaluations for the coefficients, c_i , independent of each other. However, same as single-level interpolation with HVIS, single-level quasi-interpolation has similar problems in surface reconstruction mentioned in Sect. 4, as shown in Figs. 1(d) and 2(e). In this subsection, we present a multi-level version of quasi-interpolation to overcome the problems. Two examples are shown in Figs. 1(e) and 2(f).

As stated in Sect. 4, the exact solution of the coefficients can be determined by solving the system of linear equations $f^k(\mathbf{x}) = f^{k-1}(\mathbf{x}) + \delta^k(\mathbf{x}) = 0$. We substitute $\delta^k(\mathbf{x})$ with the single-level interpolation function using a normalized basis and then rewrite the linear system as

$$\begin{aligned} & \sum_{j=1}^{n^k} c_j^k \varphi_{\rho^k}(\|\mathbf{x} - \mathbf{v}_j^k\|) \\ &= -f^{k-1}(\mathbf{x}) - \sum_{j=1}^{n^k} \langle \mathbf{n}_j^k, \nabla \varphi_{\rho^k}(\|\mathbf{x} - \mathbf{v}_j^k\|) \rangle. \end{aligned}$$

For any point \mathbf{v}_i^k , we can get the estimation of its corresponding coefficient c_i^k as

$$c_i^k = -f^{k-1}(\mathbf{v}_i^k) - \sum_{j=1}^{n^k} \langle \mathbf{n}_j^k, \nabla \varphi_{\rho^k}(\|\mathbf{v}_i^k - \mathbf{v}_j^k\|) \rangle. \quad (10)$$

5.3 Adaptive support size

Points with non-uniformities or holes are quite common in practice. From these kinds of points, as shown in Fig. 2(a), reconstruction fails when conducting the single-level interpolation and quasi-interpolation with a fixed support size for all points, see Figs. 2(b) and 2(e). Although the multi-level interpolation and quasi-interpolation methods can reconstruct surface successfully, the surfaces are not smooth in regions with sparse points (as shown in Figs. 2(c) and 2(f)).

This is because the support sizes at those sparse points are too small to have enough points in its supporting field. Enlarging the support sizes globally is not reasonable as there will be too many neighbors for the points in dense regions, which leads to an expensive computation. In order to solve this problem, we compute the support sizes in an adaptive way.

Based on the initial support size calculated by the method described in Sect. 4, we adjust the support size by considering the number of neighbors falling in a point's local support. Letting σ be the average number of points in the initial support for every point (or setting the value of σ by users), if the number of points falling in the support ρ_v of a sample v is smaller than σ , we enlarge the support size ρ_v by the factor 1.1 and check the number of points in the support again. The checking and enlarging are repeated until there are not less than σ points in the local support ρ_v of a sample point v . With adaptive support sizes, single-level interpolation and quasi-interpolation are immune to non-uniform sample points while multi-level interpolation and quasi-interpolation can reconstruct smooth surfaces that successfully overcome the problem of high non-uniformity in the given point set (see the example shown in Fig. 2). Note that σ is the parameter which can be specified by users in our approach. For non-uniform points, we find using $\sigma = 10$ can give good results.

6 Results and discussion

We evaluate our multi-level Hermite variational implicit surface interpolation (ML-HVIS-I) and quasi-interpolation (ML-HVIS-QI) methods by applying them to point sets consisting of up to ten millions of points, and comparing their accuracy and computational efficiency with several prior methods: the multi-level partition of unity and compactly supported radial basis function-based interpolation (ML-PURBF-I) [5] and quasi-interpolation (ML-PURBF-QI) [28], the screened Poisson reconstruction [16] (screened Poisson), and the multi-level partition of unity reconstruction [22] (MPU). All points are scaled into a $20 \times 20 \times 20$ bounding box. Except the screened Poisson and MPU, other methods generate mesh surfaces from reconstructed implicit surfaces by Bloomenthal's method in [29]. All statistics presented in this paper are obtained by tests running on a PC with two Intel(R) Core(TM) i7-2600K CPUs at 3.4 GHz plus 8 GBytes RAM.

6.1 Interpolation vs. quasi-interpolation

Figures 3–7 show the reconstruction results obtained by our multi-level interpolation and quasi-interpolation methods proposed in this paper. The numbers of points in these

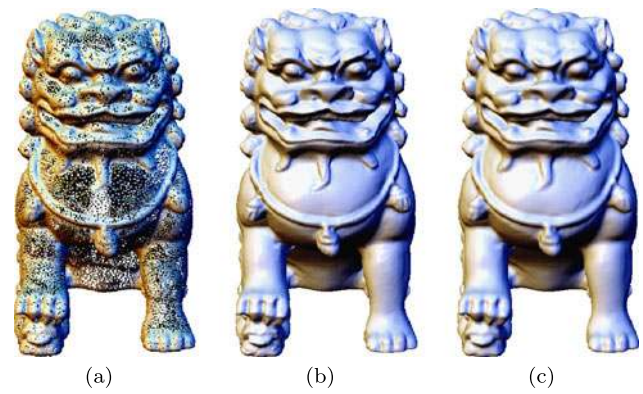


Fig. 3 Reconstruction from samples of a Chinese lion model. (a) Given 82.8k points. (b) Surface reconstructed by our ML-HVIS-I method. (c) Surface reconstructed by our ML-HVIS-QI method

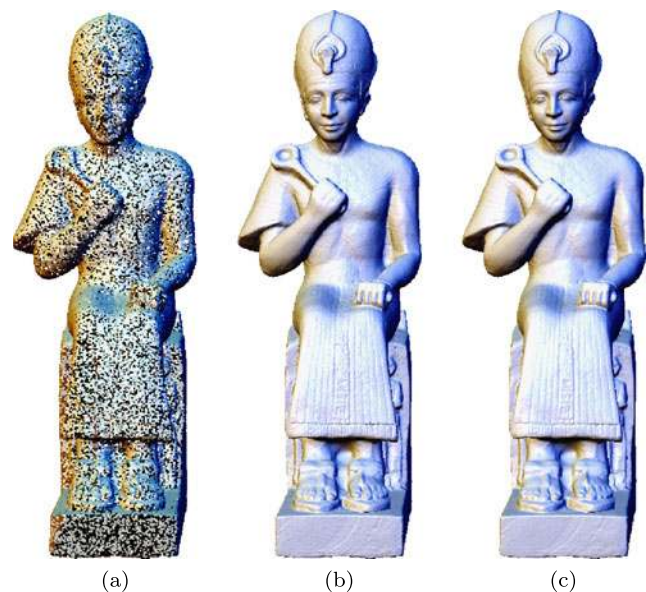


Fig. 4 Reconstruction from samples of the Ramesses model. (a) Input point cloud with 0.57 M points. Only 1/10 points are displayed in (a). (b) Surface reconstructed by our ML-HVIS-I method. (c) Surface reconstructed by our ML-HVIS-QI method



Fig. 5 Reconstruction from samples of the Buddha model. (a) Input point cloud with 2.2 M points. Only 1/20 points are displayed in (a). (b) Surface reconstructed by our ML-HVIS-I method. (c) Surface reconstructed by our ML-HVIS-QI method

examples are from 83 thousand to 10.8 million, respectively. The statistics of computing times are listed in Table 1. It is easy to find that the quasi-interpolation method is much faster than the exact interpolation method. Moreover, as the quasi-interpolation method presented can be

parallelized, the computing time can be further reduced when running on a PC with multi-cores (see Table 1). From those results shown in Figs. 3–7, the detail features are smoothed for the quasi-interpolation method when the given data has not enough points, for example the reconstruction surface shown in Fig. 3(c). But for those models with very large scale points, such as Figs. 4–7, we can hardly observe any visual difference between the reconstructed surfaces. The RMS errors listed in Table 2 prove this conclusion that the RMS error decreases when the number of points increases. From the statistics of computing time listed in Tables 1 and 2, our quasi-interpolation after parallelizing is about 10–40 times faster than the exact interpolation.

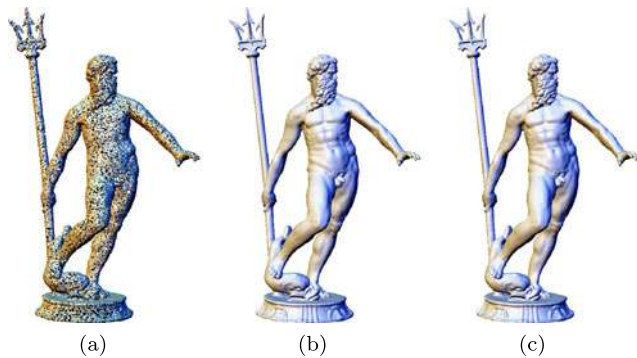


Fig. 6 Reconstruction from samples of the Neptune model. (a) Input point cloud with 5 M points. Only 1/100 points are displayed in (a). (b) Surface reconstructed by our ML-HVIS-I method. (c) Surface reconstructed by our ML-HVIS-QI method

6.2 Processing noisy point data

To process noisy data, a similar strategy as in [5, 28] is adopted here. We switch from interpolation to approximation via a regularization of the corresponding RBF interpolation matrices: instead of inverting RBF interpolation matrix \mathbf{A} , its regularization $\mathbf{A} + \lambda \mathbf{I}$ is inverted, where λ is the

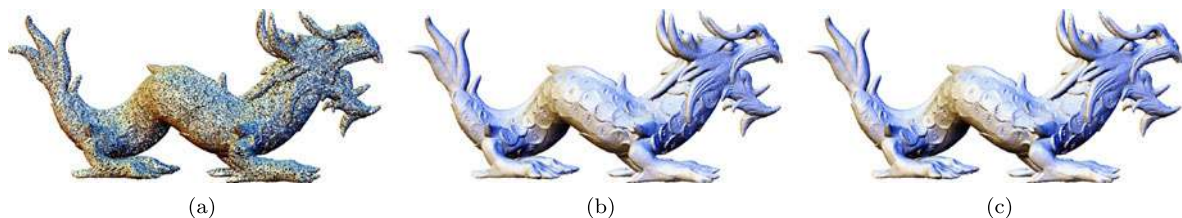


Fig. 7 Reconstruction from samples of a Chinese dragon model. (a) Input point cloud with 10.8 M points. Only 1/100 points are displayed. (b) Surface reconstructed by our ML-HVIS-I method. (c) Surface reconstructed by our ML-HVIS-QI method

Table 1 Time statistics for models with different scale points

Fig.	Model	Number of points	Multi-level interpolation time (s)	Multi-level quasi-interpolation time (s)	
				One-core	Eight-cores
3	Chinese lion	83k	5.9	2.2	0.6
4	Ramesses	570k	77.9	21.5	5.5
5	Buddha	2,159k	362.2	61.7	16
6	Neptune	4,975k	572.8	225	60
7	Chinese dragon	10,828k	2,513.5	383.7	96.3

Table 2 Runtime performance of the different reconstruction techniques and RMS errors of reconstructions

Model	Number of points	Time in seconds				RMS errors			
		ML-PURBF-I	ML-PURBF-QI	ML-HVIS-I	ML-HVIS-QI	ML-PURBF-I	ML-PURBF-QI	ML-HVIS-I	ML-HVIS-QI
Bimba	74.8k	4.7	0.7	4.2	0.4	0.0013	0.0034	0.0015	0.0018
Armadillo	173k	31.5	1.5	31	1	0.0012	0.0019	0.0013	0.0015
Raptor	1,000k	424.6	13.4	421.3	9.4	0.00042	0.0014	0.00047	0.0011

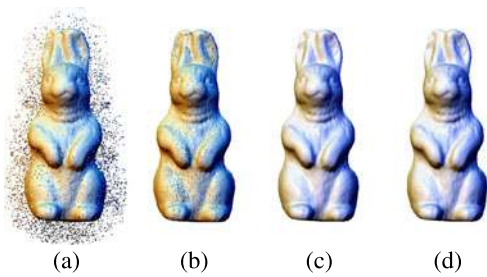


Fig. 8 Reconstruction results on a large noisy point set. (a) shows original noisy points. (b) is the resultant point set after removing outliers [30]. (c) and (d) are results from our ML-HVIS-I and ML-HVIS-QI, respectively

regularization parameter and \mathbf{I} is a unit matrix. It is useful to make the regularization parameter $\lambda = \lambda^k$ depend on the hierarchy level k . We found that setting $\lambda^k = 1.0k \cdot n^k$ can make good results. For our quasi-interpolation method, we also extend it by introducing the same regularization parameter λ^k . With this parameter λ^k , the coefficients c_i^k of our quasi-interpolation are in place of $c_i^k/(1 + \lambda^k)$.

For a point set with large noise, a preprocessing procedure (e.g., [30]) can be applied to remove the outliers. The resultant set retains only small noise. A surface can be reconstructed from it by our method proposed in this paper. An example is shown in Fig. 8. As we use the normal vectors directly in our interpolation and quasi-interpolation methods,

they are more sensitive to noises than the methods in [5, 28]. This is a limitation of our methods presented in this paper.

6.3 Comparison with ML-PURBF-I and ML-PURBF-QI

To compare our ML-HVIS-I and ML-HVIS-QI methods with ML-PURBF-I and ML-PURBF-QI methods in [5] and [28], we apply these methods to a few models (see Fig. 9). The related statistics are listed in Table 2. Figure 9 shows the reconstructions by ML-PURBF-I [5], ML-PURBF-QI [28], our ML-HVIS-I and ML-HVIS-QI. No obvious visual difference between reconstruction results of two interpolations and the original surfaces can be observed. Some details on the original surfaces are smoothed by the quasi-interpolation methods. Our ML-HVIS-QI can preserve more details than ML-PURBF-QI. Same conclusions can be found in Table 2. As shown in Table 2, where the shape approximation errors, in the form of RMS errors, are measured by the distance from the reconstructed surface to the original surface using the Metro tool [33], the reconstruction results obtained by [5] have a little smaller shape errors than our interpolation method, while our quasi-interpolation method can generate the surface with smaller shape errors than ML-PURBF-QI [28]. The local quadratic fitting somehow helps to compromise the incompatible normals in the exact interpolation procedure, but it over smooths the effects of normals in the quasi-interpolation.

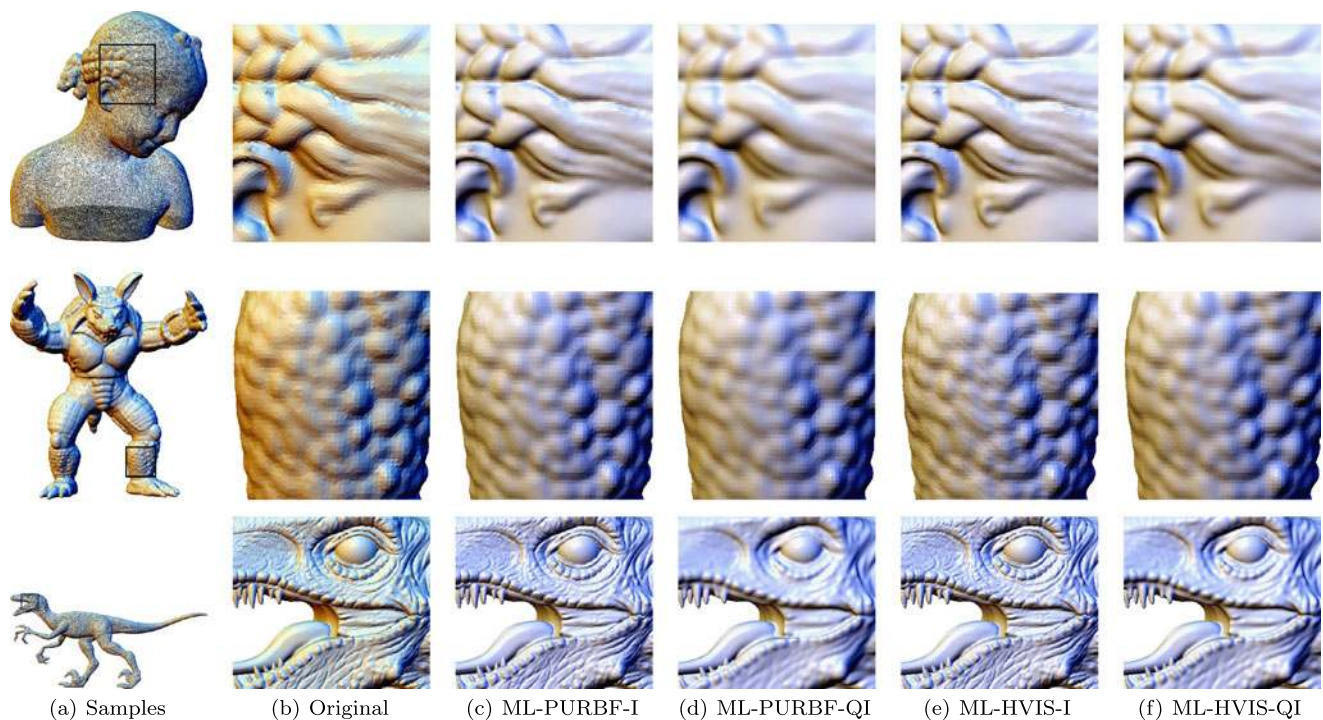


Fig. 9 Reconstruction surfaces from the points uniformly sampled on the bimba, armadillo and raptor surface models by different methods. For illustration, only 1/10 points are displayed for the raptor model

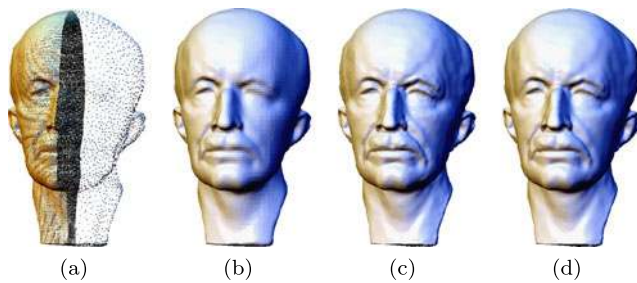


Fig. 10 Reconstructions of MaxPlanck model with non-uniform samples (a) using screened Poisson reconstruction [16] (b), our multi-level Hermite variational interpolation (c) and quasi-interpolation (d) methods with adaptive support sizes, $\sigma = 10$

For the computational efficiency, our interpolation method is a bit faster than the interpolation method in [5], and the time of performing our quasi-interpolation method is about 2/3 of the time of the method in [28]. This is because our methods do not need the local fitting procedure. In Table 2, the computing time for two quasi-interpolation methods is the running time of parallelizing the quasi-interpolation procedure on multi-cores.

In addition, about the sparsity, as a quadratic primitive described with nine floats is used for each point, ML-PURBF-I and ML-PURBF-QI need the space of $9 \sum_{k=1}^M n^k$ floats more than our corresponding methods.

6.4 Comparison with the screened Poisson and MPU method

Poisson and MPU methods are two well known techniques. We will compare our methods with them. In order to compare the reconstructed surfaces, we try to generate mesh surfaces with a similar number of triangles.

We firstly compared our results with the screened Poisson reconstruction [16] on a MaxPlanck model with highly non-uniform points, as shown in Fig. 10. The screened Poisson method [16], as shown in Fig. 10(b), can reconstruct a very smooth surface with 504,568 triangles generated with the program provided by authors of [16]. However, the details cannot be preserved well in sparse regions. Figures 10(c) and 10(d) show the result surfaces reconstructed by our ML-HVIS-I and ML-HVIS-QI methods with adaptive support sizes ($\sigma = 10$) which have more details preserved than the screened Poisson method. Two surfaces include 502,192 and 501,400 triangles, respectively. Although our adaptive ML-HVIS-I taking 10 seconds for fitting is slower than the screened Poisson method which takes 6.8 seconds, our adaptive ML-HVIS-QI uses only 1.3 seconds, which is much faster than the screened Poisson method.

We compared the results generated by our method and MPU method [22] on an Eight model, as shown in Fig. 11(a). It is a sparse model with 766 points. Because there are no sharp features on the given model, we did not

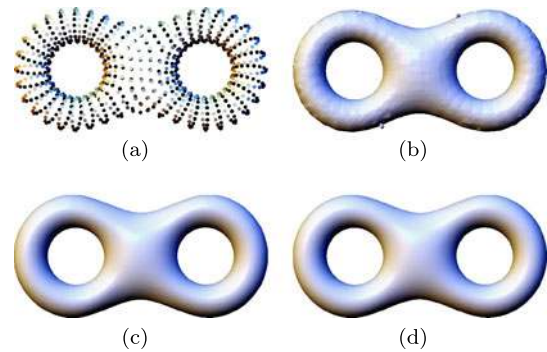


Fig. 11 Reconstructions of an Eight model with different methods: (a) the given points, (b) MPU [22], (c) ML-HVIS-I, and (d) ML-HVIS-QI with adaptive support size, $\sigma = 10$

select the sharp feature function option when performing the MPU software provided by the authors. From the results in Fig. 11, it is easy to observe the visual differences. The surface generated by MPU [22] is not smooth and has some extra unwanted parts, see Fig. 11(b). Our multi-level interpolation and quasi-interpolation methods reconstruct perfectly smooth surfaces (Figs. 11(c) and 11(d)). The quasi-interpolation adopts adaptive support size as $\sigma = 10$.

7 Conclusion

In most variational implicit surface reconstructions, normal vectors are not used as constraints directly. The non-zero constraints in the linear systems are constructed by inserting offset surface points [2, 3] or local fitting [5]. Hermite interpolation [13, 14] directly uses the normal vectors to construct the non-zero constraints which lead to a $4n \times 4n$ linear system. Pan et al. proposed a HVIS reconstruction method by incorporating the normal vectors into an optimization problem directly [6]. However, using CSRBFs results in that the method often yields unwanted artifacts and smaller step than support size in contouring in addition to the lack of extrapolation across holes. In this paper, based on [6], we present a multi-level HVIS interpolation which can overcome those problems associated with CSRBFs, and a quasi-interpolation approach for fast reconstructing an implicit surface from scattered points. Our quasi-interpolation method is simple and stable as it does not need to solve linear systems, which is a common step for almost all variational computation-based surface reconstruction methods. With adaptive support size, our quasi-interpolation-based surface reconstruction method demonstrates good performance on point sets with non-uniformity. Moreover, if only the neighbors are found, the quasi-interpolation on each point can be computed independently. This makes the surface reconstruction procedure can be easily parallelized and run on a modern PC with multi-cores. We compute the

RMS errors of our multi-level HVIS interpolation and quasi-interpolation methods for some examples instead of analyzing the approximate error in theory. Due to the page limitation, we will discuss them in another work.

There are several limitations. Our methods need to construct a multi-scale hierarchy point sets which consumes a lot of memory and computational time. Considering the recovery of sharp features, our methods blur all the sharp features on the reconstructed surfaces so that large shape approximation errors are introduced in the relevant regions. The strategy of prior work in [34] will be exploited. Due to using the normals directly, our methods are somehow sensitive to noises. For those data with large noises, our method can deal with it after applying a preprocessing step (like [30]) on the input data. In addition, a possible future work is to implement this reconstruction method on the highly parallel architecture of GPUs.

Acknowledgements This research is supported by the Natural Science Foundation of China (NSFC) grants (61173119 and 60970097), and the Research Fellowship provided by Alexander von Humboldt Foundation.

We thank the anonymous reviewers for their helpful comments, the Stanford 3D Scanning Repository for the Chinese Dragon and Armadillo models, Aim@Shape for the Neptune, Raptor, Bimbal, Eight, Chinese Lion, Ramesses, Buddha, Moai, Igea, and MaxPlanck models. We also thank Michael Kazhdan and Hugues Hoppe for providing their screened Poisson reconstruction implementation, Yutaka Ohtake and his colleagues for providing their multi-level CSRBF reconstruction and MPU implementation, P. Cignoni, C. Rocchini and R. Scopigno for providing the free Metro tool.

References

1. Dey, T.K.: Curve and Surface Reconstruction: Algorithms with Mathematical Analysis pp. 173–202. Cambridge University Press, New York (2007)
2. Carr, J., Beatson, R., Cherrie, J., Mitchell, T., Fright, W., McCallum, B., Evans, T.: Reconstruction and representation of 3D objects with radial basis function. In: Proceedings of the 28th Annual Conference on Computer Graphics and Interactive Techniques (SIGGRAPH'2001), pp. 67–76 (2001)
3. Turk, G., O'Brien, J.F.: Modeling with implicit surfaces that interpolate. *ACM Trans. Graph.* **21**(4), 855–873 (2002)
4. Morse, B.S., Yoo, T.S., Rheingans, P., Chen, D.T., Subramanian, K.R.: Interpolating implicit surfaces from scattered surfaces data using compactly supported radial basis functions. In: Shape Modeling International 2001, Genova, Italy, pp. 89–98 (2001)
5. Ohtake, Y., Belyaev, A., Seidel, H.-P.: 3d scattered data interpolation and approximation with multilevel compactly supported RBFs. *Graph. Models* **67**, 150–165 (2005)
6. Pan, R., Meng, X., Whangbo, T.: Hermite variational implicit surface reconstruction. *Sci. China, Ser. F* **52**(2), 308–315 (2009)
7. Wendland, H.: Piecewise polynomial, positive definite and compactly supported radial basis functions of minimal degree. *Adv. Comput. Math.* **4**, 389–396 (1995)
8. Dey, T.K., Dyer, R., Wang, L.: Localized Cocone surface reconstruction. *Comput. Graph.* **35**(3), 483–491 (2011)
9. Amenta, N., Choi, S., Kolluri, R.: The power crust. In: Proceedings of 6th ACM Symposium on Solid Modeling, pp. 249–266. ACM, New York (2001)
10. Dey, T.K., Goswami, S.: Provable surface reconstruction from noisy samples. *Comput. Geom.* **35**(1), 124–141 (2006)
11. Kolluri, R., Shewchuk, J.R., O'Brien, J.F.: Spectral surface reconstruction from noisy point clouds. In: Proceedings of the 2004 Eurographics/ACM Siggraph Symposium on Geometry Processing, pp. 11–21. ACM, New York (2004)
12. Tobor, I., Reuter, P., Schlick, C.: Reconstructing multi-scale variational partition of unity implicit surfaces with attributes. *Graph. Models* **68**(1), 25–41 (2006)
13. Walder, C., Schölkopf, B., Chapelle, O.: Implicit surface modelling with a globally regularised basis of compact support. *Comput. Graph. Forum* **25**(3), 635–644 (2006)
14. Macedo, I., Gois, J.P., Velho, L.: Hermite radial basis functions implicit. *Comput. Graph. Forum* **30**(1), 27–42 (2011)
15. Alliez, P., Cohen-Steiner, D., Tong, Y., Desbrun, M.: Voronoi-based variational reconstruction of unoriented point sets. In: Proceedings of the Fifth Eurographics Symposium on Geometry Processing, pp. 39–48. Eurographics Association Aire-la-Ville, Switzerland (2007)
16. Kazhdan, M., Hoppe, H.: Screened Poisson surface reconstruction. *ACM Trans. Graph.* (2013)
17. Calakli, F., Taubin, G.: SSD: smooth signed distance surface reconstruction. *Comput. Graph. Forum* **30**(7), 1993–2002 (2011)
18. Hoppe, H., DeRose, T., Duchamp, T., McDonald, J., Stuetzle, W.: Surface reconstruction from unorganized points. In: Proceedings of the 19th Annual Conference on Computer Graphics and Interactive Techniques (SIGGRAPH '92), pp. 71–78. ACM, New York (1992)
19. Alexa, M., Behr, J., Cohen-Or, D., Fleishman, S., Levin, D., Silva, T. C.: Point set surfaces. In: Proceedings of the Conference on Visualization '01, pp. 21–28. IEEE Computer Society, Washington (2001)
20. Guennebaud, G., Gross, M.: Algebraic point set surface. *ACM Trans. Graph.* **26**(3), 23.1–23.9 (2007)
21. Amenta, N., Kil, Y.: Defining point-set surfaces. *ACM Trans. Graph.* **23**(3), 264–270 (2004)
22. Ohtake, Y., Belyaev, A., Alexa, M., Turk, G., Seidel, H.-P.: Multi-level partition of unity implicit. *ACM Trans. Graph.* **22**(3), 463–470 (2003)
23. Debaos, C.: Degree of approximation by superpositions of a sigmoidal function. *Approx. Theory Its Appl.* **9**(3), 17–28 (1993)
24. Mhaskar, H.N., Michelli, C.A.: Approximation by superposition of sigmoidal and radial basis functions. *Adv. Appl. Math.* **13**(3), 350–373 (1992)
25. Lianas, B., Sainz, F.J.: Constructive approximate interpolation by neural networks. *J. Comput. Appl. Math.* **188**(2), 283–308 (2006)
26. Zhang, W., Wu, Z.: Shape-preserving MQ-B-Splines quasi-interpolation. In: Proceedings Geometric Modeling and Processing, pp. 85–92 (2004)
27. Han, X., Hou, M.: Quasi-interpolation for data fitting by the radial basis functions. In: Advances in Geometric Modeling and Processing. Lecture Notes in Computer Science, vol. 4975, pp. 541–547 (2008)
28. Liu, S., Wang, C.: Quasi-interpolation for surface reconstruction from scattered data with radial basis functions. *Comput. Aided Geom. Des.* **29**(7), 435–447 (2012)
29. Bloomenthal, J.: Polygonization of implicit surfaces. *Comput. Aided Geom. Des.* **5**(4), 341–355 (1988)
30. Liu, S., Chan, K.-C., Wang, C.: Iterative consolidation of unorganized point clouds. *IEEE Comput. Graph. Appl.* **32**(3), 70–83 (2012)
31. Schall, O., Samozino, M.: Surface from scattered points: a brief survey of recent developments. In: Falcidieno, B., Magnenat-Thalmann, N. (eds.) 1st International Workshop on Semantic Virtual Environment, pp. 138–147 (2005)

32. Shepard, D.: A two-dimensional interpolation function for irregularly-spaced data. In: Proceedings of the 1968 23rd ACM National Conference, pp. 517–524. ACM, New York (1968)
33. Cignoni, P., Rocchini, C., Scopigno, R.: Metro: measuring error on simplified surfaces. *Comput. Graph. Forum* **17**(2), 167–174 (1998)
34. Wang, J., Yu, Z., Zhu, W., Cao, J.: Feature-Preserving Surface Reconstruction from Unoriented, Noisy Point Data. *Comput. Graph. Forum* **32**(1), 164–176 (2013)



Shengjun Liu is an associate professor in the School of Mathematics and Statistics in Central South University, China. His research interests include geometric modeling, reverse engineering, computer graphics and compute aided geometric design. Liu has a DEng in computer science and technology from Zhejiang University. Contact him at shjliu.cg@gmail.com.



Guido Brunneth is a full professor of computer graphics in the Chemnitz University of Technology's Computer Science Department. He also directs the Institute of Mechatronics, a private research institute affiliated with the university. Brunneth has a Ph.D. in computer science from the University of Kaiserslautern and a diploma in mathematics from the University of Dortmund. His research interests include geometric modeling, CAD/CAM applications, virtual reality and virtual humans. Contact him at brunneth@cs.tu-chemnitz.de.



Jun Wang received the B.S. and Ph.D. degrees both in mechanical engineering from Nanjing University Aeronautics and Astronautics (China) in 2002 and 2007, respectively. He was a postdoctoral scholar at the University of California-Davis from 2008 to 2009. Since then he has been a research associate at the University of Wisconsin-Milwaukee. His research interests are geometric modeling and processing, in particular, mesh segmentation and processing. Contact him at davis.wjun@gmail.com.